Eur. Phys. J. D (2015)
DOI: 10.1140/epjd/e2015-60427-6

THE EUROPEAN PHYSICAL JOURNAL D

Regular Article

Theoretical study of true-muonium $\mu^+\mu^-$ formation in muon collision processes $\mu^- + \mu^+e^-$ and $\mu^+ + p\mu^-$

True-muonium $\mu^+\mu^-$ formation in $\mu^- + \mu^+e^-$ and $\mu^+ + p\mu^-$

Kazuhiro Sakimoto[a]

Institute of Space and Astronautical Science, Japan Aerospace Exploration Agency, 3-1-1 Yoshinodai, Chuo-ku, Sagamihara, Kanagawa 252-5210, Japan

Received 21 July 2015 / Received in final form 30 September 2015
Published online (Inserted Later) – © EDP Sciences, Società Italiana di Fisica, Springer-Verlag 2015

Abstract. Formation processes of true muonium ($\mu^+\mu^-$) atoms are investigated theoretically 1) for negative-muon (μ^-) collisions with a muonium (Mu = μ^+e^-) atom (i.e., $\mu^- + \mu^+e^- \to \mu^+\mu^- + e^-$) and 2) for positive-muon (μ^+) collisions with a muonic hydrogen ($p\mu^-$) atom (i.e., $\mu^+ + p\mu^- \to \mu^+\mu^- + p$). The calculations are carried out by using two different types of approaches: one, applied to the $\mu^- + e^-\mu^+$ system where electron emission plays an important role, is a semiclassical (SC) method, in which the radial distance between the negative and positive muons is treated as a classical variable, and the remaining degrees of freedom are described by quantum mechanics. The other is a classical-trajectory Monte Carlo (CTMC) method, in which all the degrees of freedom are described by classical mechanics. The formation and ionization (or dissociation) cross sections and the state distributions of produced true-muonium atoms are presented.

1 Introduction

Atomic bound states of a muon-antimuon pair $\mu^+\mu^-$ are called *true muonium* (or also known as *di-muonium*) [1–3]. Since a muon is 207 times heavier than an electron, the hydrogenic $\mu^+\mu^-$ atom has a deep ground ($1s$) state energy of -1.41 keV, and a very small Bohr radius of mere 512 fm. Due to this compactness, although the $\mu^+\mu^-$ atom has not yet been observed experimentally, its spectroscopic study is expected to play an important role in a QED test [1–5]. A muonic hydrogen $p\mu^-$ atom is also an interesting compact system, and recently experiments of measuring the Lamb shift and $2s$ hyperfine splitting of $p\mu^-$ have become feasible [6,7]. However, in comparing between theory and experiment, one must consider a hadronic effect especially due to a finite proton size [6–9]. In this respect, the $\mu^+\mu^-$ atom is a purely leptonic system, and is ideally suited for the QED test. The possibility of producing $\mu^+\mu^-$ atoms (via virtual photons on nuclei, positron-electron annihilation, etc.) in high-energy collider experiments has been discussed in several papers [3,10–13]. Unfortunately, it does not seem very likely that the $\mu^+\mu^-$ atoms manufactured by high-energy colliders will be directly tractable for further performing high-precession spectroscopic measurements.

Recently, a source of muonium (Mu = μ^+e^-) atoms with a high vacuum yield becomes available in low temperature conditions [14,15]. Furthermore, many efforts have been made to obtain low-energy μ^- beams [16–18]. Under these circumstances, as part of the Ultra Slow Muon project at J-PARC MUSE [19], it has been suggested that the $\mu^+\mu^-$ atoms may be efficiently produced by using atomic collision processes of a negative muon and a Mu atom, i.e.,

$$\mu^- + \mu^+e^- \to \mu^+\mu^- + e^-. \tag{1}$$

In planning such experiments, detailed information on the reaction (1) becomes important needless to say, though it cannot be obtained sufficiently at the present time [20]. In the sense that the system is composed of an electron and two heavy particles with opposite charges, the reaction (1) is closely analogous to $p\bar{p}$ formation in $\bar{p} + \mathrm{H}$ (or $p\mu^-$ formation in $\mu^- + \mathrm{H}$), for which detailed theoretical studies have been already progressed [21–23].

Although no experimental plan has been arranged so far to use muon exchange in atomic collisions of a positive muon and a muonic hydrogen atom, i.e.,

$$\mu^+ + p\mu^- \to \mu^+\mu^- + p, \tag{2}$$

this reaction may be also expected to be an efficient means of producing the $\mu^+\mu^-$ atoms. As described before, the $p\mu^-$ atom is really utilized for testing QED [6,7]. Low-energy μ^+ beams are available by inducing the ionization of the Mu atoms with lasers [15,24]. If the $p\mu^-$ atom is in the ground state (i.e., the principal quantum number $n = 1$), the reaction (2) is highly endoergic (-1.12 keV), and is of absolutely no use for producing the $\mu^+\mu^-$ atoms. On the other hand, if $n \geq 2$, the reaction (2) becomes exoergic ($\geq$0.774 keV), and can take

[a] e-mail: sakimoto@isas.jaxa.jp

place even at low collision energies. The $p\mu^-$ atoms are produced after stopping and capture of negative muons in hydrogen media. It is noteworthy that highly-excited states ($n \gtrsim 15$) of the $p\mu^-$ atoms are primarily produced in elementary collision processes such as $\mu^- + \mathrm{H}$ [22,23]. The density of matter for stopping muons is usually so high that the highly-excited states rapidly cascade down to lower ones [25–27]. In the absence of collisions with surroundings, however the highly-excited states could remain unchanged for a long time. Furthermore, the availability of sufficiently long-lived $p\mu^-$ atoms in the $2s$ state has been experimentally established [28]. Thus, it is quite conceivable that the excited states of $p\mu^-$ atoms will be available as a target in the reaction (2).

The present paper makes a theoretical study of the two types of the $\mu^+\mu^-$-formation processes (1) and (2) by means of reasonably reliable methods. The ionization ($\rightarrow \mu^+ + \mu^- + e^-$) and dissociation ($\rightarrow \mu^+ + \mu^- + p$) processes are also investigated. Electron emission dominates the reaction dynamics in $\mu^- + \mu^+e^-$, and accordingly the calculation for this system is carried out by using a semiclassical (SC) method, in which the radial distance between μ^+ and μ^- is treated as a classical variable, and the other degrees of freedom are described by quantum mechanics. The SC method was applied to $\bar{p} + \mathrm{H}$ and $\mu^- + \mathrm{H}$ [21,23], which are allied to the present $\mu^- + \mu^+e^-$ system. The reliability of the SC method was demonstrated for $\bar{p} + \mathrm{H}$ and $\mu^- + \mathrm{H}$ by comparing the results with accurate quantum mechanical (QM) results [21,23] (for other theoretical methods, see Ref. [22]). One may expect that the SC method is appropriate also for the investigation of the reaction (1). Although the accurate QM method could be applied to the reaction (1), its calculation encounters double-continuum difficulties at energies above the ionization threshold. On the other hand, the SC method can be employed at energies both below and above the ionization threshold. For the $\mu^+ + p\mu^-$ system, a classical-trajectory Monte Carlo (CTMC) method is introduced. The application of the CTMC method to the Coulomb three-body collision problem was examined in references [29–31]. The reaction (2) is similar to positronium (e^+e^-) formation in $e^+ + \mathrm{H}$ or $e^- + \bar{\mathrm{H}}$. QM calculations have been carried out for this system [32]. However, since muons are much heavier than electrons, the application of the QM treatment to the reaction (2) would not be so easy. CTMC calculations were carried out for the $e^- + \bar{\mathrm{H}}$ system [33,34], and the results agree well with experimental results of the $e^+ + \mathrm{H}$ system [35]. Since muons can be regarded as a heavy particle, the CTMC method is expected to work much better for the $\mu^+ + p\mu^-$ system. In the present paper, an additional CTMC calculation is carried out also for $\mu^- + \mu^+e^-$, though an electron is not a heavy particle.

2 Semiclassical method

The SC method is applied to the $\mu^+\mu^-$ formation and the ionization in $\mu^- + \mu^+e^-$ collisions. The time-dependent Schrödinger equation in the SC method is given by [21,23]

$$i\frac{\partial}{\partial t}\Psi^{JM}(\hat{\mathbf{R}}, \mathbf{r}, t) = \tilde{H}\Psi^{JM}(\hat{\mathbf{R}}, \mathbf{r}, t), \tag{3}$$

where (J, M) are the total angular momentum quantum numbers of the $\mu^- + \mu^+e^-$ system, $\mathbf{R} = (R, \hat{\mathbf{R}})$ is the position vector of μ^- from μ^+, and $\mathbf{r} = (r, \hat{\mathbf{r}})$ is that of e^- from μ^+. Here and in the following, atomic units are used unless otherwise stated. The Hamiltonian $\tilde{H}$ in equation (3) is:

$$\tilde{H} = \frac{\tilde{\mathbf{L}}^2}{2m_R R^2} + \frac{\tilde{\mathbf{p}}^2}{2m_r} + V, \tag{4}$$

where $\tilde{\mathbf{L}}$ is the $\mu^+\mu^-$ angular momentum operator, $\tilde{\mathbf{p}}$ is the electronic momentum operator, m_R and m_r are the reduced masses of $\mu^- + \mu^+$ and $e^- + \mu^+$, respectively, and V is the interaction. The total wave function $\Psi^{JM}(\hat{\mathbf{R}}, \mathbf{r}, t)$ can be written as [21,23]

$$\Psi^{JM}(\hat{\mathbf{R}}, \mathbf{r}, t) = \frac{1}{r}\sum_{\lambda}\left(\frac{2J+1}{4\pi}\right)^{1/2} D^J_{-M-\lambda}(\hat{\mathbf{R}})\psi^{J\lambda}(\mathbf{r}, t), \tag{5}$$

where $D^J_{M\lambda}(\hat{\mathbf{R}})$ is the Wigner rotation matrix element. The parameter R is taken, as was done in previous SC studies [21,23], to represent the classical radial motion governed by the Born-Oppenheimer potential of the $\mu^- + \mu^+e^-$ system [36]. In the $\mu^- + \mu^+e^-$ collisions, the μ^+e^- atom is assumed to be initially in the $1s$ state.

The hydrogenic $\mu^+\mu^-$ state is identified by (N, L), which are the principal and angular momentum quantum numbers. The distribution of the kinetic energy ε and angular momentum l of emitted electrons for a specified L can be given by [23]

$$\frac{dP^J_{Ll}}{d\varepsilon} = \frac{1}{m_r}\mathrm{Im}\left[(A^J_{Ll})^*\frac{dA^J_{Ll}}{dr}\right]_{r=r_0}, \tag{6}$$

where r_0 is taken to be sufficiently large, and

$$A^J_{Ll}(r, \varepsilon) = \frac{1}{\sqrt{2\pi}}\sum_{\lambda} U^{Jl}_{L\lambda}\int e^{i\varepsilon t}\left\langle Y_{l\lambda}\middle|\psi^{J\lambda}(t)\right\rangle_r dt, \tag{7}$$

with the spherical harmonics $Y_{l\lambda}(\hat{\mathbf{r}})$ and

$$U^{Jl}_{L\lambda} = \left(\frac{2L+1}{2J+1}\right)^{1/2}(L0l\lambda|J\lambda). \tag{8}$$

In the present study, the probability of the μ^- capture to form $\mu^+\mu^-$ in the (N, L) state is defined by:

$$P^J_{NL} = \sum_l\int_{\varepsilon_1}^{\varepsilon_2}\frac{dP^J_{Ll}}{d\varepsilon}d\varepsilon = m_R\sum_l\int_{N-1/2}^{N+1/2}\frac{dP^J_{Ll}}{d\varepsilon}\frac{d\mathfrak{N}}{\mathfrak{N}^3}, \tag{9}$$

where $\varepsilon_{1,2}$ are the electron energies corresponding to $\mathfrak{N} = N \pm \frac{1}{2}$ through the conservation of energy [23]

$$E_{\mathrm{tot}} = \varepsilon - \frac{m_R}{2\mathfrak{N}^2} = E - \frac{m_r}{2}, \tag{10}$$

with E being the center-of-mass (CM) collision energy of $\mu^- + \mu^+e^-$. The cross section for the formation of the (N, L) state is given by:

$$\sigma^{\rm SC}_{\mu^+\mu^-}(N,L) = \frac{\pi}{2m_R E}\sum_J (2J+1)P^J_{NL}. \quad (11)$$

The (N, L)-state distribution is defined as:

$$F^{\rm SC}(N,L) = \sigma^{\rm SC}_{\mu^+\mu^-}(N,L)/\sigma^{\rm SC}_{\mu^+\mu^-}, \quad (12)$$

where

$$\sigma^{\rm SC}_{\mu^+\mu^-} = \sum_{NL}\sigma^{\rm SC}_{\mu^+\mu^-}(N,L) \quad (13)$$

is the total formation cross section. If the electron energy is $0 < \varepsilon < E_{\rm tot}$, this case corresponds to the (break-up) ionization. Then, the ionization cross section becomes

$$\sigma^{\rm SC}_{\rm ion} = \frac{\pi}{2m_R E}\sum_{JLl}(2J+1)\int_0^{E_{\rm tot}}\frac{dP^J_{Ll}}{d\varepsilon}d\varepsilon. \quad (14)$$

For the numerical calculation of $\psi^{J\lambda}(\mathbf{r}, t)$ in equation (5), a grid-representation technique based on zero-points of orthogonal polynomials was employed. The details were given in reference [23]. The Chebyshev polynomials with 530 zero-points were adopted for the range of $0 \le r \le 80a_0$, and the complete absorbing potential was applied to avoid the reflection from the outer boundary. The Legendre or Gegenbauer polynomials with 3 zero-points were adopted for the polar angle of $\mathbf{r}$. The channels of $|\lambda| \le 1$ were coupled. For reference, these parameters provide the Mu($1s$) energy -13.37 eV (the accurate value is -13.54 eV) and the adiabatic polarizability 4.717 in atomic units (the accurate value is 4.5). The maximum total angular momenta considered in the collision calculations are, e.g., $J_{\rm max} = 9$ for $E = 1$ eV, $J_{\rm max} = 22$ for $E = 10$ eV, $J_{\rm max} = 50$ for $E = 50$ eV, $J_{\rm max} = 71$ for $E = 100$ eV, etc.

3 Classical-trajectory Monte Carlo method

For the system A + BC = $\mu^+ + p\mu^-$ or $\mu^- + e^-\mu^+$, the CTMC method is employed to investigate the $\mu^+\mu^-$ formation. Let $(\mathbf{Q}, \mathbf{q})$ denote the Jacobi coordinates associated with the A + BC arrangement: $\mathbf{Q}$ being the position vector of A from BC and $\mathbf{q}$ being that of C from B. The classical equations of motion are

$$\frac{d\mathbf{Q}}{dt} = \frac{\mathbf{P}}{m_Q}, \quad \frac{d\mathbf{P}}{dt} = -\frac{\partial U}{\partial \mathbf{Q}}, \quad (15)$$

$$\frac{d\mathbf{q}}{dt} = \frac{\mathbf{p}}{m_q}, \quad \frac{d\mathbf{p}}{dt} = -\frac{\partial U}{\partial \mathbf{q}}, \quad (16)$$

where m_Q and m_q are the corresponding reduced masses, and U is the interaction. A set of equations (15) and (16) were solved by a Runge-Kutta method. The numerical details of the CTMC calculation were described in reference [37]. The initial energy of the hydrogenic BC atom having the principal quantum number n is given by $-m_q/(2n^2)$. In reference [37], the initial angular momentum of the target was given as a fixed value. In the present study, no special value is specified for the initial angular momentum j of BC, and a uniform distribution is assumed for j^2 [38], which has the range

$$0 \le \mathrm{j}^2 \le \mathrm{j}^2_{\rm max} = n^2. \quad (17)$$

The cross sections for $\mu^+\mu^-$ formation and dissociation (or ionization) are calculated from

$$\sigma^{\rm CTMC}_{\mu^+\mu^-} = \pi b^2_{\rm max}\frac{I_{\mu^+\mu^-}}{I}, \quad (18)$$

$$\sigma^{\rm CTMC}_{\rm dis(ion)} = \pi b^2_{\rm max}\frac{I_{\rm dis(ion)}}{I}, \quad (19)$$

where $b_{\rm max}$ is the largest value of the impact parameter b considered in the calculation, I is the total number of trajectories calculated, and $I_{\mu^+\mu^-/\rm dis/ion}$ is the number of events satisfying a criteria for formation/dissociation/ionization. It was confirmed that no reaction took place for $b \ge b_{\rm max}$. The state of the isolated $\mu^+\mu^-$ atoms in the trajectory calculation is identified by the classical angular momentum $\mathfrak{L}$ and the classical energy

$$\mathfrak{E}_{\mu^+\mu^-} = \frac{m_R}{2}\left(\frac{d\mathbf{R}}{dt}\right)^2 - \frac{1}{R}. \quad (20)$$

The associated quantum numbers (N, L) that are integer may be given by the relations [39]

$$\left[(N-1)\left(N-\frac{1}{2}\right)N\right]^{1/3} \le \mathfrak{N} < \left[N\left(N+\frac{1}{2}\right)(N+1)\right]^{1/3}, \quad (21)$$

$$L < \frac{N}{\mathfrak{N}}\mathfrak{L} \le L+1, \quad (22)$$

where

$$\mathfrak{N} = \left(\frac{m_R}{2|\mathfrak{E}_{\mu^+\mu^-}|}\right)^{1/2}. \quad (23)$$

Then, the (N, L)-state distribution is calculated by:

$$F^{\rm CTMC}(N,L) = \frac{I_{\mu^+\mu^-}(N,L)}{I_{\mu^+\mu^-}}, \quad (24)$$

where $I_{\mu^+\mu^-}(N, L)$ is the number of trajectories resulting in the formation of the (N, L) state.

The CTMC calculations with $I = 5000$–$15\,000$ were carried out. The values of $b_{\rm max}$ were chosen as $b_{\rm max} = 3.0a_0$–$6.64a_0$ for $\mu^- + \mu^+e^-(n = 1)$, $b_{\rm max} = 0.09a_0$–$0.2a_0$ for $\mu^+ + p\mu^-(n = 2)$, $b_{\rm max} = 0.5a_0 - 1.0a_0$ for $\mu^+ + p\mu^-(n = 5)$, $b_{\rm max} = 2.5a_0 - 3.5a_0$ for $\mu^+ + p\mu^-(n = 10)$, $b_{\rm max} = 4.0a_0 - 10.0a_0$ for $\mu^+ + p\mu^-(n = 15)$, and $b_{\rm max} = 6.0a_0 - 15.0a_0$ for $\mu^+ + p\mu^-(n = 20)$. To ensure the numerical reliability, the CTMC calculations were tested for $p\mu^-$ formation in μ^- + H and for $p\bar{p}$ formation

in $\bar{p}$ + H with a somewhat smaller number of trajectories ($I = 1000$). The deviations in the cross section from the previous CTMC calculation of Cohen (μ^- + H) [30] are 2.5% at $E = 10.9$ eV and 0.48% at $E = 16.3$ eV, and those from the CTMC calculation of Schultz ($\bar{p}$ + H) [31] are 3.5% at $E = 8.16$ eV and 1.8% at $E = 13.6$ eV. These deviations are within the statistical errors.

4 Results

4.1 μ^- + μ^+e^- collisions

In this section, the results are presented for the $\mu^- + \mu^+ e^-$ collision system. Using the SC method, the reaction cross sections and the $\mu^+\mu^-$-state distributions were calculated at collision energies $E = 1-100$ eV. Throughout this paper, the collision energy E is represented in the CM frame. The CTMC method was also applied to this system, and the comparison was made between the two methods.

The $\mu^+\mu^-$-formation and ionization cross sections in the low-, intermediate-, and high-energy regions are plotted as a function of the CM energy E together in Figure 1. Since the $\mu^+\mu^-$ formation is exoergic, its cross section increases with decreasing E even at low energies. The ionization channel becomes open only at energies above the threshold $E = m_r/2$. For all the reaction channels, the CTMC cross sections are overall much larger than the SC ones. The same holds true with regard to the μ^- + H and $\bar{p}$ + H systems [21,40]. As was expected, the classical treatment of the electron would be deficient. However, if one aims at observing only the qualitative behavior of the cross sections, it can be said that the CTMC method is acceptable.

As seen in the middle part of Figure 1, the formation and ionization channels are competitive, and their cross sections change places rapidly within a narrow range (ΔE) of energies above the ionization threshold $E = m_r/2$. The energy range ΔE is equal to the highest energy $\varepsilon = \varepsilon_0$ that can be carried away by the emitted electrons [23]. The present SC and CTMC calculations offer $\Delta E \sim 15$ eV. For comparison, the middle part of Figure 1 also includes the CTMC cross sections calculated by Cohen for $p\mu^-$ formation in μ^- + H [30]. The CTMC cross section of μ^- + H is smaller than the present CTMC result of μ^- + Mu, and the energy range ΔE seems to be slightly smaller for μ^- + H. Another previous CTMC study [41] shows that the energy range for $p\bar{p}$ formation in $\bar{p}$ + H is $\Delta E \sim 5$ eV, which is much smaller than that of μ^- + H. The reduced-mass ratio of $\bar{p}$ + H, μ^- + H and μ^- + Mu is about 9 : 2 : 1. For the system of a negatively-charged particle and a hydrogen isotope, it may be expected that the formation can take place at higher energies above the ionization threshold (i.e., ΔE becomes larger) if the reduced mass of the collision system is getting smaller. Since the ionization energy practically vanishes at small distances (R) in these systems [22,36,42], the effective transition energy in the electron emission may be just equal to the electron kinetic energy ε. Then, the so-called Massey criterion [43] suggests that the emitted electrons mostly have $\varepsilon \sim 1/\tau$,

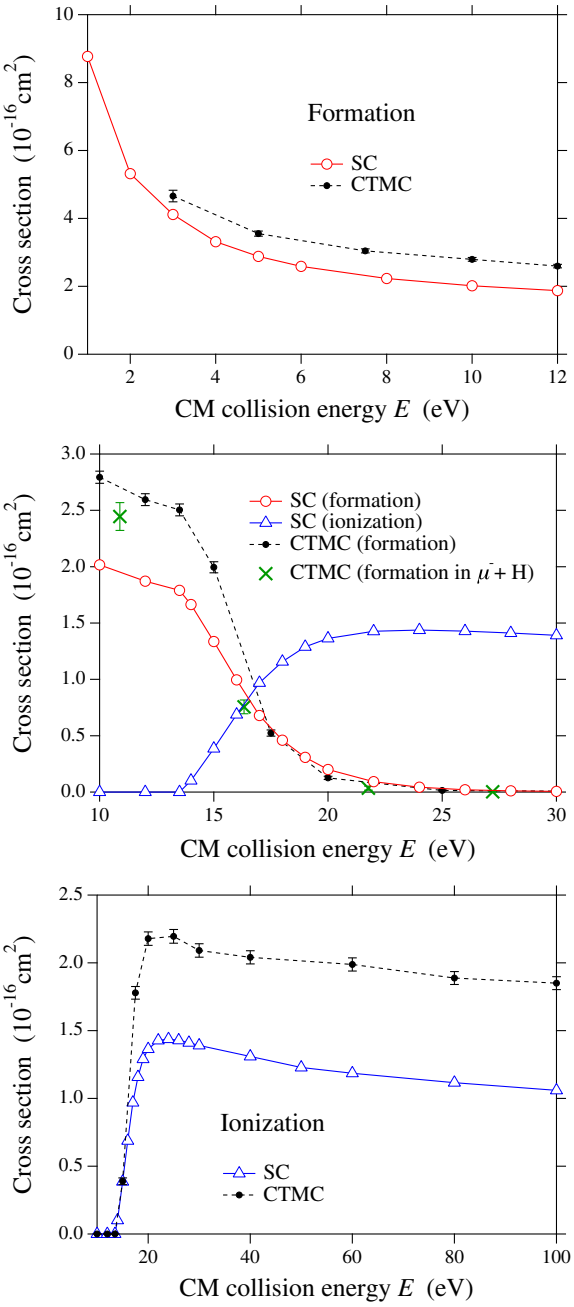

Fig. 1. Cross sections for $\mu^+\mu^-$ formation and ionization in $\mu^- + \mu^+ e^-$ collisions, calculated by the SC and CTMC methods. CTMC cross sections for $p\mu^-$ formation in μ^- + H obtained by Cohen [30] are also plotted in the middle figure. The collision energy E is represented in the CM frame.

with τ being the collision time. Since this relation implies that $\varepsilon_0 \propto 1/\tau$, one can obtain (for the same collision energy E) $\Delta E \simeq \varepsilon_0 \propto (\text{reduced mass})^{1/2}$, which seems to be in accord with the present finding.

The $\mu^+\mu^-$ formation in μ^- + Mu offers a remarkable resemblance to associative electron detachment in the H^- + H system [44], i.e.,

$$H^- + H \rightarrow H_2 + e^-. \qquad (25)$$

Also for this reaction, a rapid decrease in the cross section was observed at collision energies just above the detachment threshold [44]. In this case, the break-up detachment ($\rightarrow \mathrm{H} + \mathrm{H} + e^-$) competes with the reaction (25). An isotope effect was investigated by comparing the cross sections between the $\mathrm{H}^- + \mathrm{H}$ and $\mathrm{D}^- + \mathrm{D}$ systems [45]: Although no notable isotope effect was found, the energy range corresponding to the present ΔE seemed to be slightly (but non-negligibly) smaller for $\mathrm{D}^- + \mathrm{D}$ than for $\mathrm{H}^- + \mathrm{H}$. The origin of the only slight difference may be the same as that for the $\mu^- + \mathrm{Mu}$ and $\mu^- + \mathrm{H}$ systems: The reduced-mass ratio between the isotope systems is ~ 2 for the both cases of the associative detachment ($\mathrm{D}^- + \mathrm{D}$ and $\mathrm{H}^- + \mathrm{H}$) and the present type of formation reaction ($\mu^- + \mathrm{H}$ and $\mu^- + \mathrm{Mu}$).

Figure 2 shows the state distributions $F(N, L)$ calculated by the SC method at CM collision energies $E = 5, 10$, and 15 eV. The distribution is visualized as a brightness scale image. At first glance, an image feature changes drastically with E. Generally, the distribution is shifted to higher quantum numbers with increasing E. The produced states can have very high N up to ∞, but are limited to somewhat low L. Interestingly, the image feature at $E = 10$ eV is very similar to that of the QM calculation for μ^-+H at $E = 10$ eV [46] except for the related range of quantum numbers: Since the reduced mass of $p\mu^-$ is about twice as large as that of $\mu^+\mu^-$, it is natural that different values of quantum numbers are involved in $\mu^- + \mathrm{Mu}$ and $\mu^- + \mathrm{H}$.

Figure 3 shows the state distributions defined by:

$$F(N) = \sum_L F(N, L), \quad F(L) = \sum_N F(N, L), \qquad (26)$$

and compares the results between the SC and CTMC methods. The CTMC method is in good agreement with the SC method for the L distribution $F(L)$, and offers a much narrower distribution for $F(N)$. In Figure 4, the average quantum numbers defined by:

$$\bar{N} = \sum_N N\, F(N), \quad \bar{L} = \sum_L L\, F(L) \qquad (27)$$

are plotted as a function of E. For both $\bar{L}$ and $\bar{N}$, good agreement can be obtained between the two methods. As was sometimes assumed in previous studies, one might expect that the most probable state of produced $\mu^+\mu^-$ were estimated by the condition of energy matching, i.e., $N \sim \sqrt{m_R/m_r} \simeq 10$. Figure 4 shows that this is the case only at very-low collision energies. The average quantum number $\bar{N}$ actually has significant E dependence, and becomes very large at high E. Instead, it is empirically true that the average quantum number $\bar{L}$ takes a value of $\sim\sqrt{m_R/m_r}$ at high collision energies. Thus, the simple evaluation formula $\sqrt{m_R/m_r}$ should be used as the most probable value of N only if E is very low and otherwise as that of L.

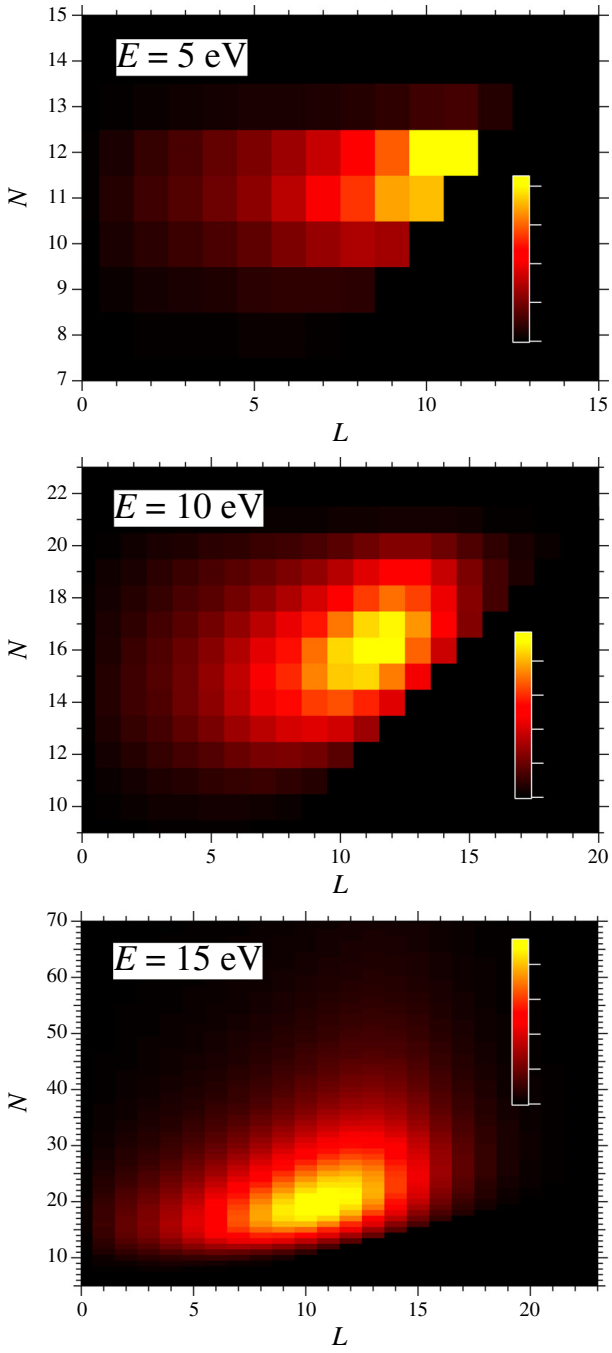

Fig. 2. (N, L)-state distributions $F(N, L)$ in $\mu^- + \mu^+e^-$ collisions at the CM collision energies $E = 5, 10$, and 15 eV, calculated by the SC method.

4.2 $\mu^+ + \mathrm{p}\mu^-$ collisions

For the $\mu^+ + p\mu^-(n)$ collision system, the CTMC method was used to investigate the $\mu^+\mu^-$ formation and dissociation processes. The calculations were carried out for several initial states n between 2 and 20. Related energies at which the reaction processes prominently take place differ depending on the initial state n. A rough indication of such energies is given by the dissociation energy of $p\mu^-(n)$, i.e., $D_n = m_q/(2n^2) = 2.53 \times 10^3/n^2$ eV.

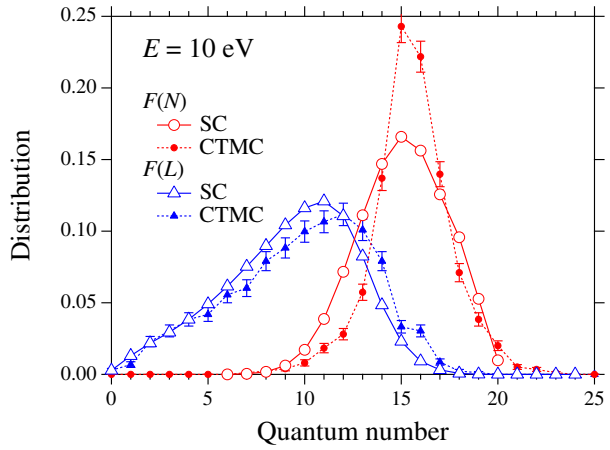

Fig. 3. N- and L-state distributions $F(N)$ and $F(L)$ in $\mu^- + \mu^+e^-$ collisions at the CM collision energy $E = 10$ eV, calculated by the SC and CTMC methods.

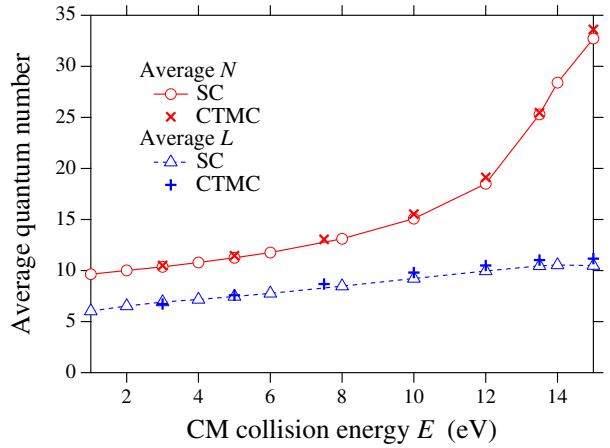

Fig. 4. Average quantum numbers $\bar{N}$ and $\bar{L}$ in $\mu^- + \mu^+e^-$ collisions, calculated by the SC and CTMC methods. The collision energy E is represented in the CM frame.

Figure 5 shows the reaction cross sections as a function of the CM collision energy E for the initial states $n = 2, 5$, and 15. With increasing n, the cross sections become large, and the related energies become low. Since the formation reaction is exoergic for $n \geq 2$, its cross section increases with decreasing E. The energy dependence is overall similar for all the cases of $n \geq 2$, though a notable shoulder structure appears at $E \sim D_n$ for $n = 2$. In contrast to the $\mu^- + \mu^+e^-$ system, it turns out that the formation can occur even at high energies much above the dissociation threshold (i.e., $E \gg D_n$).

Figure 6 shows the N-state distribution $F(N)$ for the initial states $n = 2, 5$, and 15. It is seen that the $\mu^+\mu^-$ states with higher N can be produced as E increases. However, the position $N = N_0$ of the distribution peak remains mostly unchanged with E. In the $\mu^+ + p\mu^-$ system, the condition of energy matching offers $N \sim n\sqrt{m_Q/m_q} = 0.746n$, which is always close to N_0 regardless of the values of n and E. This result is quite different from that of the $\mu^- + \mu^+e^-$ system.

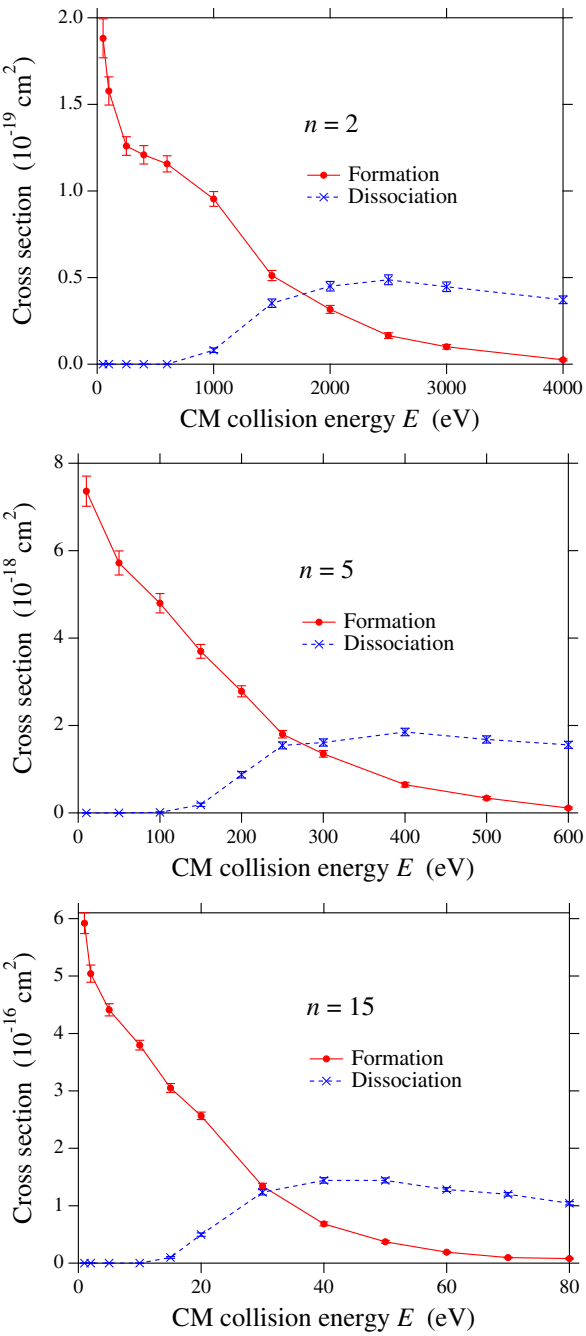

Fig. 5. Cross sections for $\mu^+\mu^-$ formation and dissociation in $\mu^+ + p\mu^-(n)$ with $n = 2, 5$, and 15, calculated by the CTMC method. The collision energy E is represented in the CM frame.

The similarity in the E dependence observed in Figure 5 suggests that the cross sections for different n might be scaled to each other. For hydrogenic atoms, the average radius and the binding energy both have a scale factor n^2. In Figure 7, accordingly the scaled cross sections $\sigma_{\mu^+\mu^-}/n^4$ and $\sigma_{\rm dis}/n^4$ are plotted as a function of the scaled energy n^2E for various initial states of $n = 2$–20. It seems that the plotted data are mostly approximated by a single smooth curve, except for the data

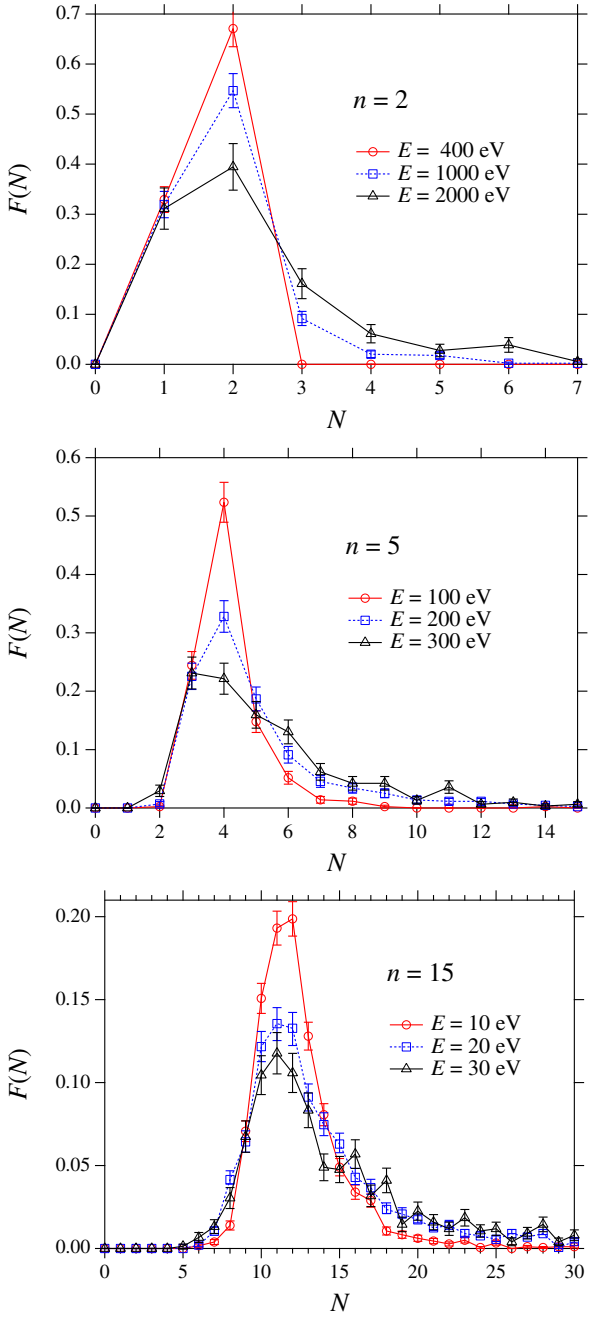

Fig. 6. N-state distributions $F(N)$ in $\mu^+ + p\mu^-(n)$ with $n = 2, 5$, and 15, calculated by the CTMC method.

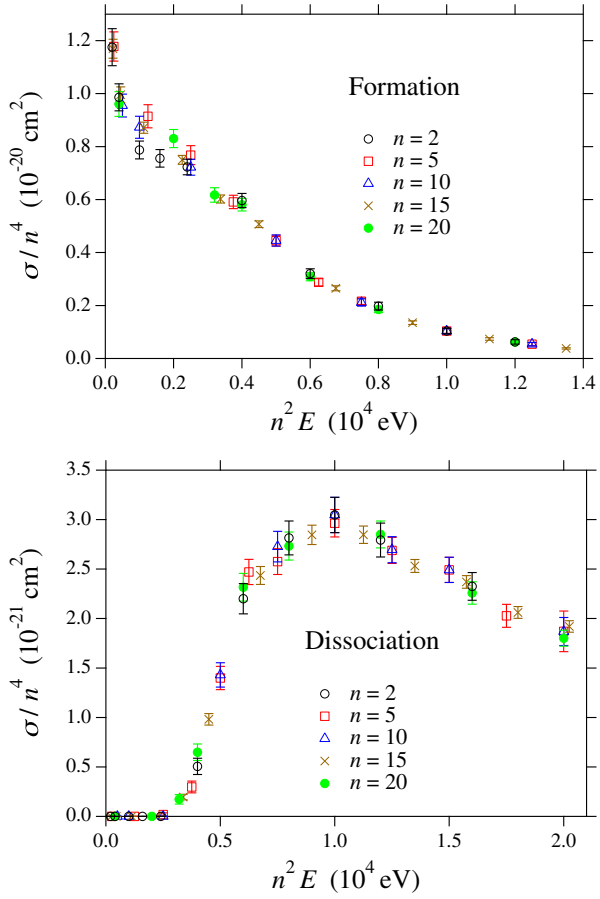

Fig. 7. Scaled formation cross sections $\sigma_{\mu^+\mu^-}/n^4$ and scaled dissociation cross sections $\sigma_{\rm dis}/n^4$ plotted as a function of n^2E in $\mu^+ + p\mu^-(n)$ with $n = 2, 5, 10, 15$, and 20, calculated by the CTMC method. The collision energy E is represented in the CM frame.

of the $n = 2$ formation cross sections just below $n^2E \sim n^2D_n = 2.53 \times 10^3$ eV. Analogous n-scaling laws can be established for the cross sections of collision processes involving highly-excited Rydberg atoms [47–51]. By using the scaling law found in the present study, the reaction cross sections of the $\mu^+ + p\mu^-$ collisions can be easily estimated for any initial state $n \geq 2$ and any energy E. For reference, the scaled formation cross section $y = \sigma_{\mu^+\mu^-}/n^4$ in units of 10^{-20} cm^2 can be roughly evaluated by a simple exponential fitting $y = A\exp(-Bx)$ with $x = n^2E$ in units of eV, where the coefficients are given by $A = 1.09, B = 1.79 \times 10^{-4}$ if $200 \leq x < 4000$, and $A = 1.90, B = 2.92 \times 10^{-4}$ if $x \geq 4000$.

5 Summary and discussion

The present paper has investigated the reaction processes of true-muonium $\mu^+\mu^-$ formation in different two types of atomic collisions: 1) between a negative muon μ^- and a muonium atom μ^+e^- and 2) between a positive muon μ^+ and a muonic hydrogen atom $p\mu^-$. The theoretical calculations have been carried out with use of the SC method for describing the dynamics dominated by electron emission in the $\mu^- + \mu^+e^-$ system, and with use of the CTMC method for describing the muon exchange dynamics in the $\mu^+ + p\mu^-$ system.

It has been found that the $\mu^+\mu^-$ formation cannot take place in the $\mu^- + \mu^+e^-$ system unless $E < 30$ eV. Hence, when one tries to produce the $\mu^+\mu^-$ atoms in collision experiments of $\mu^- + \mu^+e^-$, it is absolutely necessary that μ^- beams available in experiments [16–18] contain a sufficient amount of <30 eV energy components (in the CM frame).

In contrast to the $\mu^- + \mu^+ e^-$ system, the $\mu^+\mu^-$ formation has been found to be able to take place at much higher energies in the $\mu^+ + p\mu^-$ system. This finding may be an encouraging result for experimentalists. The essential requirement for the practical use of the $\mu^+ + p\mu^-$ collisions is that the $p\mu^-$ atoms in excited ($n \geq 2$) states can be extracted and become available as a target. The experimental evidence of the existence of long-lived $p\mu^-$ atoms in the $2s$ state [28] may be a favorable outlook for manufacturing the $\mu^+\mu^-$ atoms. It has been established conveniently for the $\mu^+ + p\mu^-$ system that the formation cross section satisfies a useful scaling law with respect to the principal quantum number n of $p\mu^-$.

The $\mu^+\mu^-$ principal quantum number determined by the condition of energy matching may be assumed to be the most probable state produced in the $\mu^+\mu^-$ formation. This is always true in the $\mu^+ + p\mu^-$ system, and is not so except at very-low energies in the $\mu^- + \mu^+ e^-$ system. In the latter case, much higher states are produced with increasing energy. In the experiments of the $\mu^+\mu^-$ formation using $\mu^- + \mu^+ e^-$, unless the related collision energies are much below the ionization threshold, care may be needed because the $\mu^+\mu^-$ atoms in very-high states can be easily destroyed by further collisions with surroundings. Such collisional effects were disadvantageous also in producing antiprotonic helium ($He^+\bar{p}$) atoms [52,53].

Finally, let us examine the effect of a finite lifetime ($\sim$2 μs) of the muon in detecting $\mu^+\mu^-$ atoms. The experimental production of $\mu^+\mu^-$ atoms should be accomplished within this lifetime. The formation rate of $\mu^+\mu^-$ in the reaction (1) is given by:

$$\frac{dN_{\mu^+\mu^-}}{dt} = v\sigma_{\mu^+\mu^-} n_{\mu^-} N_{\mathrm{Mu}}, \tag{28}$$

where $N_{\mu^+\mu^-}$ is the number of $\mu^+\mu^-$, v is the collision velocity, n_{μ^-} is the number density of μ^-, and N_{Mu} is the number of Mu. Its inverse is a time required for producing one $\mu^+\mu^-$ atom, and hence should be shorter than the muon lifetime. The typical current experimental condition of J-PARK MUSE is [19]: $vn_{\mu^-} \sim 0.64 \times 10^7$ cm^{-2} s^{-1} and $N_{\mathrm{Mu}} \sim 0.3 \times 10^6$. Inserting these values and $\sigma_{\mu^+\mu^-} \sim 10^{-16}$ cm^2 obtained in this study offers

$$\left(\frac{dN_{\mu^+\mu^-}}{dt}\right)^{-1} \sim 5 \times 10^3 \text{ s}, \tag{29}$$

which is much longer than the muon lifetime. Unfortunately, the current experimental condition is not yet sufficient to detect $\mu^+\mu^-$ atoms. Further efforts are expected to be made for realizing the experimental plan to use the reaction (1) [18,19]. It is not certain whether the $\mu^+\mu^-$ atoms produced in the reaction (2) can be experimentally detected. In this respect, a recent experimental study [54,55] is very encouraging: the rate constants for the chemical reaction process involving muonic helium ($He^+\mu^-$) atoms, i.e., $He^+\mu^- + H_2 \rightarrow He^+\mu^- H + H$, have been measured, and namely the muonic atom is actually available to investigate its collision process within the muon lifetime. This study shows promising advances also for the $\mu^+\mu^-$ detection via the reaction (2).

References

1. D. Owen, W.W. Repko, Phys. Rev. A **5**, 1570 (1972)
2. J. Malenfant, Phys. Rev. D **36**, 863 (1987)
3. S.J. Brodsky, R.F. Lebed, Phys. Rev. Lett. **102**, 213401 (2009)
4. U.D. Jentschura, G. Soff, V.G. Ivanov, S.G. Karshenboim, Phys. Rev. A **56**, 4483 (1997)
5. H. Lamm, R.F. Lebed, J. Phys. G **41**, 125003 (2014)
6. R. Pohl, A. Antognini, F. Nez, F.D. Amaro, F. Biraben, J.M.R. Cardoso, D.S. Covita, A. Dax, S. Dhawan, L.M.P. Fernandes, A. Giesen, T. Graf, T.W. Hänsch, P. Indelicato, L. Julien, C. Kao, P. Knowles, E. Le Bigot, Y. Liu, J.A.M. Lopes, L. Ludhova, C.M.B. Monteiro, F. Mulhauser, T. Nebel, P. Rabinowitz, J.M.F. dos Santos, L.A. Schaller, K. Schuhmann, C. Schwob, D. Taqqu, J.F.C.A. Veloso, F. Kottmann, Nature **466**, 213 (2010)
7. A. Antognini, F. Nez, K. Schuhmann, F.D. Amaro, F. Biraben, J.M.R. Cardoso, D.S. Covita, A. Dax, S. Dhawan, M. Diepold, L.M.P. Fernandes, A. Giesen, T. Graf, A.L. Gouvea, T.W. Hänsch, P. Indelicato, L. Julien, C.Y. Kao, P. Knowles, F. Kottmann, E.O.L. Bigot, Y.W. Liu, J.A.M. Lopes, L. Ludhova, C.M.B. Monteiro, F. Mulhauser, T. Nebel, P. Rabinowitz, J.M.F. dos Santos, L.A. Schaller, C. Schwob, D. Taqqu, J.F.C.A. Veloso, J. Vogelsang, R. Pohl, Science **339**, 417 (2013)
8. U.D. Jentschura, Ann. Phys. **326**, 500 (2011)
9. E. Borie, Ann. Phys. **327**, 733 (2012)
10. E. Holvik, H.A. Olsen, Phys. Rev. D **35**, 2124 (1987)
11. I.E. Ginzburg, U.D. Jentschura, S.G. Karshenboim, F. Krauss, V.G. Serbo, G. Soff, Phys. Rev. C **58**, 3565 (1998)
12. N. Arteaga-Romero, C. Carimalo, V.G. Serbo, Phys. Rev. A **62**, 032501 (2000)
13. A. Banburski, P. Schuster, Phys. Rev. D **86**, 093007 (2012)
14. A. Antognini, P. Crivelli, T. Prokscha, K.S. Khaw, B. Barbiellini, L. Liszkay, K. Kirch, K. Kwuida, E. Morenzoni, F.M. Piegsa, Z. Salman, A. Suter, Phys. Rev. Lett. **108**, 143401 (2012)
15. G.A. Beer, Y. Fujiwara, S. Hirota, K. Ishida, M. Iwasaki, S. Kanda, H. Kawai, N. Kawamura, R. Kitamura, S. Lee, W. Lee, G.M. Marshall, T. Mibe, Y. Miyake, S. Okada, K. Olchanski, A. Olin, H. Ohnishi, Y. Oishi, M. Otani, N. Saito, K. Shimomura, P. Strasser, M. Tabata, D. Tomono, K. Ueno, E. Won, K. Yokoyama, Prog. Theor. Exp. Phys. **2014**, 091C01 (2014)
16. P. DeCecco, P. Hauser, D. Horváth, F. Kottmann, L.M. Simons, D. Taqqu, Nucl. Instrum. Meth. A **394**, 287 (1997)
17. N. Kawamura, T. Masuda, P. Strasser, Y. Miyake, J. Phys.: Conf. Ser. **225**, 012026 (2010)
18. K. Nagamine, JPS Conf. Proc. **2**, 010403 (2014)
19. K. Nagamine, JPS Conf. Proc. **2**, 010001 (2014)
20. Y. Miyake (private communication)
21. K. Sakimoto, Phys. Rev. A **66**, 032506 (2002)
22. J.S. Cohen, Rep. Prog. Phys. **67**, 1769 (2004)
23. K. Sakimoto, Phys. Rev. A **84**, 032501 (2011)
24. D. Taqqu, Phys. Procedia **17**, 216 (2011)
25. V. Bystritsky, W. Czapliński, N. Popov, Eur. Phys. J. D **5**, 185 (1999)
26. T.S. Jensen, V.E. Markushin, Eur. Phys. J. D **21**, 271 (2002)

27. L. Ludhova, F.D. Amaro, A. Antognini, F. Biraben, J.M.R. Cardoso, C.A.N. Conde, A. Dax, S. Dhawan, L.M.P. Fernandes, T.W. Hänsch, V.W. Hughes, P. Indelicato, L. Julien, P.E. Knowles, F. Kottmann, Y.-W. Liu, J.A.M. Lopes, C.M.B. Monteiro, F. Mulhauser, F. Nez, R. Pohl, P. Rabinowitz, J.M.F. dos Santos, L.A. Schaller, C. Schwob, D. Taqqu, J.F.C.A. Veloso, Phys. Rev. A **75**, 040501 (2007)
28. R. Pohl, H. Daniel, F.J. Hartmann, P. Hauser, F. Kottmann, V.E. Markushin, M. Mühlbauer, C. Petitjean, W. Schott, D. Taqqu, P. Wojciechowski-Grosshauser, Phys. Rev. Lett. **97**, 193402 (2006)
29. R.E. Olson, A. Salop, Phys. Rev. A **16**, 531 (1977)
30. J.S. Cohen, Phys. Rev. A **27**, 167 (1983)
31. D.R. Schultz, Phys. Rev. A **40**, 2330 (1989)
32. P. Comini, P.-A. Hervieux, New J. Phys. **15**, 095022 (2013)
33. A.M. Ermolaev, Hyperfine Interact. **44**, 375 (1988)
34. R.J. Whitehead, J.F. McCann, I. Shimamura, Phys. Rev. A **64**, 023401 (2001)
35. J.P. Merrison, H. Bluhme, J. Chevallier, B.I. Deutch, P. Hvelplund, L.V. Jørgensen, H. Knudsen, M.R. Poulsen, M. Charlton, Phys. Rev. Lett. **78**, 2728 (1997)
36. R.F. Walls, R. Herman, H.W. Milnes, J. Mol. Spectrosc. **4**, 51 (1960)
37. K. Sakimoto, J. Phys. B **37**, 2255 (2004)
38. R. Abrines, I.C. Percival, Proc. Phys. Soc. **88**, 861 (1966)
39. R.E. Olson, Phys. Rev. A **24**, 1726 (1981)
40. K. Sakimoto, Phys. Rev. A **70**, 064501 (2004)
41. J.S. Cohen, Phys. Rev. A **36**, 2024 (1987)
42. E. Fermi, E. Teller, Phys. Rev. **72**, 399 (1947)
43. H.S.W. Massey, Rep. Prog. Phys. **12**, 248 (1949)
44. K.A. Miller, H. Bruhns, J. Eliášek, M. Čížek, H. Kreckel, X. Urbain, D.W. Savin, Phys. Rev. A **84**, 052709 (2011)
45. K.A. Miller, H. Bruhns, M. Čížek, J. Eliášek, R. Cabrera-Trujillo, H. Kreckel, A.P. O'Connor, X. Urbain, D.W. Savin, Phys. Rev. A **86**, 032714 (2012)
46. X.M. Tong, T. Shirahama, K. Hino, N. Toshima, Phys. Rev. A **75**, 052711 (2007)
47. K.B. MacAdam, R. Rolfes, D.A. Crosby, Phys. Rev. A **24**, 1286 (1981)
48. I.L. Beigman, V.S. Lebedev, Phys. Rep. **250**, 95 (1995)
49. K.B. MacAdam, E. Horsdal-Pedersen, J. Phys. B **36**, R167 (2003)
50. K. Sakimoto, J. Phys. B **38**, 3447 (2005)
51. M. Ward, T. Cooper, Z. Wilbanks, K. Cornelius, Phys. Rev. A **85**, 064701 (2012)
52. M. Hori, J. Eades, R.S. Hayano, T. Ishikawa, J. Sakaguchi, T. Tasaki, E. Widmann, H. Yamaguchi, H.A. Torii, B. Juhász, D. Horváth, T. Yamazaki, Phys. Rev. Lett. **89**, 093401 (2002)
53. M. Hori, J. Eades, E. Widmann, T. Yamazaki, R.S. Hayano, T. Ishikawa, H.A. Torii, T. von Egidy, F.J. Hartmann, B. Ketzer, C. Maierl, R. Pohl, M. Kumakura, N. Morita, D. Horváth, I. Sugai, Phys. Rev. A **70**, 012504 (2004)
54. D.G. Fleming, D.J. Arseneau, O. Sukhorukov, J.H. Brewer, S.L. Mielke, G.C. Schatz, B.C. Garrett, K.A. Peterson, D.G. Truhlar, Science **331**, 448 (2011)
55. D.G. Fleming, D.J. Arseneau, O. Sukhorukov, J.H. Brewer, S.L. Mielke, D.G. Truhlar, G.C. Schatz, B.C. Garrett, K.A. Peterson, J. Chem. Phys. **135**, 184310 (2011)